



Evaluation of local heating in Doppler-broadening thermometry based on cavity ring-down spectroscopy

Luigi Moretti ^{*}, Antonio Castrillo , and Livio Gianfrani

Department of Mathematics and Physics, University of Campania “Luigi Vanvitelli”, Viale Lincoln 5, 81100 Caserta, Italy



(Received 25 June 2019; published 2 October 2019)

We report on an optical and thermal model that allows one to quantify the local heating effect in a cavity ring-down spectroscopy (CRDS) experiment. The effect is due to the intracavity absorption of the laser radiation propagating inside the optical cavity, when this latter is filled with an absorbing gas. The local heating generates a temperature profile into the volume probed by the laser radiation, thus leading to a systematical deviation in temperature measurements by means of Doppler-broadening gas thermometry. Exploiting the representation of the cavity as a linear system for the electric field in the frequency domain, we were able to determine the spatial and temporal behaviors of the heating source and solve the inhomogeneous Fourier heat transfer equation using the method of the Green’s functions. The local heating effect is strongly dependent on several parameters characterizing the CRDS experiment, including the geometrical size of the cavity, the two mirrors’ reflectivity and loss, the absorption coefficient of the intracavity gaseous medium, the incident power, and the intracavity beam waist. The dynamical behavior of the gas temperature was calculated in three experimental regimes, depending on the laser switch-on time interval as compared to the cavity decay time and heat diffusion characteristic time. In the worst case, the local heating provides a systematical shift in Doppler broadening thermometry of about one part per million.

DOI: [10.1103/PhysRevA.100.042501](https://doi.org/10.1103/PhysRevA.100.042501)

I. INTRODUCTION

On May 20, 2019, the most significant revision to the International System of Units (SI) came into force. It results from new measurement methods, developed in the past two decades, including those that use quantum phenomena. The new SI is based on a set of definitions linked to fundamental constants of physics. In particular, the new kelvin (the unit of thermodynamic temperature) is defined in terms of a fixed value of the Boltzmann constant, namely, $k_B = 1.380649 \times 10^{-23}$ J/K. Reviews of the experiments that led to this value are reported in Refs. [1,2]. Research efforts of the international community working in the field of primary gas thermometry are being devoted to the implementation of the redefined kelvin [3]. Within this framework, Doppler-broadening thermometry (DBT) is widely recognized as a valuable method for the primary realization of the unit kelvin, even though it has not yet reached the same level of accuracy of more consolidated techniques, such as acoustic gas thermometry [4] and dielectric constant gas thermometry [5]. DBT consists of determining the Doppler width from the shape of a given atomic or molecular line, as observed from a highly accurate laser-based absorption-spectroscopy experiment under a linear regime of radiation-matter interaction [6]. Recently, there have been interesting DBT implementations based on cavity ring-down spectroscopy (CRDS) [6,7]. Unlike direct detection of laser transmission from a conventional absorption cell, the high sensitivity of CRDS enables one to work at low pressures (of the order of 1 Pa) so that it is

possible to limit the influence of collisions, thus simplifying the spectral analysis. This is of the utmost importance to reduce the uncertainty associated to the choice of the line-shape model that has been one of the major hurdles for a low-uncertainty implementation of DBT. By recording the spectrum of C_2H_2 at 787 nm, the study of [7] demonstrates a statistical uncertainty of 6 parts per million (ppm), with the potential of approaching the 1 ppm limit with a proper choice of molecular target and spectral region. This is confirmed in Ref. [8], whose temperature determinations on a CO_2 gaseous sample at $1.578 \mu m$ show a statistical uncertainty of 8 ppm. The uncertainty budget of both papers did not consider the local heating that results from the intracavity light absorption. This effect may lead to significant systematical deviations due to the enhancement of the laser power inside a resonant high-finesse optical cavity. The present paper is aimed at investigating this issue. Of the two CRDS experiments, the attention was focused on the one with the highest precision, namely, the work dealing with the near-infrared spectrum of acetylene [7].

II. THEORETICAL MODEL

A. Thermal model

In Fig. 1, a sketch of the optical cavity is reported. We consider the case of an open symmetric stable resonator constituting of two circular mirrors with reflection coefficient r_1 and r_2 and transmission coefficient t_1 and t_2 , respectively. The mirrors’ radius is ρ_0 and the cavity length is L . We denote with $T = T_0 + \delta T(\mathbf{r}, t)$ the temperature in the position \mathbf{r} at time t , while T_0 is the temperature on the walls of the cavity

*luigi.moretti@unicampania.it

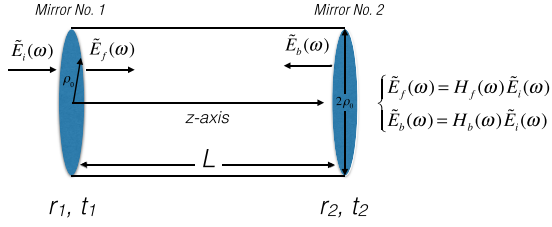


FIG. 1. Conceptual scheme of the optical cavity and representation of the electric fields propagating inside the cavity.

and δT is the temperature variation due to the optical power absorbed by the gas sample, W_{abs} , which is assumed to be completely transformed into thermal energy. The evaluation of the perturbation induced by the local heating on the temperature determination is given by $\delta T/T_0$, setting T_0 at 300 K. The thermal diffusion inside the optical cavity is ruled by the inhomogeneous heat-conduction equation with Dirichlet boundary condition ($\delta T = 0$ on the boundary surface, S), that is,

$$\left[\frac{1}{\mathcal{D}} \frac{\partial}{\partial t} - \Delta \right] \delta T(\mathbf{r}, t) = \frac{1}{\kappa} W_{\text{abs}}(\mathbf{r}, t), \quad (1)$$

$$\delta T(\mathbf{r}, t)|_S = 0,$$

where \mathcal{D} and κ are the thermal diffusivity and the thermal conductivity of the gas sample, respectively.

The solution is obtained by the time convolution of the Green's function of Eq. (1) with the thermal source, namely,

$$\delta T(\mathbf{r}, t) = \frac{1}{\kappa} \int_{V_c} d^3 \mathbf{r}' \int_{-\infty}^{+\infty} dt' G(\mathbf{r}, \mathbf{r}', t - t') W_{\text{abs}}(\mathbf{r}', t'), \quad (2)$$

where $G(\mathbf{r}, \mathbf{r}', t - t')$ is the solution of the Eq. (1) when a point source is located at \mathbf{r}' at the time t' . The geometry of the system leads us to choose a cylindrical coordinate system with the origin at the center of mirror 1 and the z axis coincident with the cavity axis. Therefore, the Green's function, taking into account the boundary condition, is given by [9]

$$G(\rho, z, \rho', z', t - t') = \frac{\mathcal{D}}{2\pi} \theta(t - t') \sum_{\substack{n=1 \\ s=0}}^{\infty} e^{-\mathcal{D}\beta_{\text{ns}}(t-t')} \\ \times \phi_n(z) \phi_n(z') \psi_s(\rho) \psi_s(\rho'), \quad (3)$$

where $\theta(t - t')$ is the Heaviside step function; $\phi_n(z)$ and $\psi_s(\rho)$ are the orthonormal and complete sets of eigenfunctions of the longitudinal and radial parts of the Laplacian operator, respectively; and β_{ns} 's are the sums of the corresponding eigenvalues:

$$\phi_n(z) = \sqrt{\frac{2}{L}} \sin\left(\frac{n\pi z}{L}\right), \quad (4)$$

$$\psi_s(\rho) = \frac{\sqrt{2}}{\rho_0 J_1(l_s)} J_0\left(\frac{l_s \rho}{\rho_0}\right), \quad (5)$$

$$\beta_{\text{ns}} = \left(\frac{l_s}{\rho_0}\right)^2 + \left(\frac{n\pi}{L}\right)^2. \quad (6)$$

Here, $J_0(x)$ and $J_1(x)$ are the Bessel functions and l_s are the zeros of $J_0(x)$. It is worth noting that Eq. (2) describes the response of the system to a heating source W_{abs} by means of the response at a point source. Finally, the temperature inside the volume (V_L) probed by the laser beam can be evaluated as the spatial average of $\delta T(\mathbf{r}, t)$:

$$\delta T_{\text{av}}(t) = \frac{1}{V_L} \int_{V_L} d^3 \mathbf{r} \delta T(\mathbf{r}, t). \quad (7)$$

B. Optical model

The electric fields playing a fundamental role in the definition of the heat source W_{abs} are reported in Fig. 1. We denote the incident field (at $z = 0$) as

$$E_i(\rho, t) = E_0 g_i(t) e^{-i\omega_c t - \frac{\rho^2}{w_0^2}}, \quad (8)$$

that is the time-domain complex representation of a linearly polarized Gaussian laser field incident on mirror 1. In this equation, ω_c is the laser carrier frequency and w_0 is the spot size of the laser beam. The function $g_i(t)$ describes the pulse envelope, that, in typical CRDS experiments, is a rectangular function with a time duration Δ , defined as the switch-on time of the laser. The frequency spectrum of the incident field, $\tilde{E}_i(\rho, \omega)$, has been found via Fourier transformation of $E_i(\rho, t)$. Its general form is

$$\tilde{E}_i(\rho, \omega) = E_0 \tilde{g}_i(\omega - \omega_c) e^{-\frac{\rho^2}{w_0^2}}. \quad (9)$$

The cavity eigenmodes of an open resonator constitute sourceless configurations of the electromagnetic field that satisfy Maxwell's relations and the boundary conditions imposed by the mirrors. As is well known, these modes are uniquely denoted as transverse electromagnetic (TEM) modes labeled with eigenfrequency ω_{qmn} . The excited eigenmodes depend on the overlap of the spectral content of the incident field with cavity eigenfrequency structure and on the extent to which the transverse profile of the incident beam overlaps with the cavity transverse modes [10]. Considering that the transverse size of the incident beam is very small with respect to the mirror radius and that the spectral content of the incident beam includes only the fundamental eigenfrequency of the cavity, it can be assumed that only the fundamental Gaussian mode (TEM_{q00}) with eigenfrequency $\omega_{q00} = 2\pi q/\tau_r$, where $\tau_r = 2L/c$ is the cavity round-trip time, is excited. The cavity eigenmodes propagate unchanged after one round trip inside the cavity, except for a small intensity loss. Thanks to this property, we can write the fields emerging from the two mirrors by considering all cavity round trips:

$$\tilde{E}_f(\rho, \omega) = \frac{\epsilon t_1}{1 - r_1 r_2 e^{i\delta}} \tilde{E}_i(\rho, \omega) = H_f(\omega) \tilde{E}_i(\rho, \omega), \quad (10)$$

$$\tilde{E}_b(\rho, \omega) = \frac{\epsilon t_1 r_2 e^{i\delta/2}}{1 - r_1 r_2 e^{i\delta}} \tilde{E}_i(\rho, \omega) = H_b(\omega) \tilde{E}_i(\rho, \omega), \quad (11)$$

where $\delta = (\omega/c + i\alpha/2)2L$ is the phase shift due to a single round trip of the electric field, α is the absorption coefficient of the gas sample at the frequency ω , and ϵ is the coupling coefficient between the incident field and the fundamental cavity mode. For an excitation frequency near the longitudinal transverse mode of any longitudinal mode, ω_{q00} ($|\Delta\omega|\tau_r =$

$|\omega - \omega_{q00}| \tau_r \ll 1$), and for an optical thin sample ($\alpha L \ll 1$), it is possible to simplify Eqs. (10) and (11) so that the response functions $H_f(\omega)$ and $H_b(\omega)$ are closely approximated by the familiar dispersion functions:

$$H_f(\omega) \simeq A_f \frac{1}{\gamma_f - i\Delta\omega}, \quad (12)$$

$$H_b(\omega) \simeq -A_b \frac{\gamma_b + i\Delta\omega}{\gamma_f - i\Delta\omega}, \quad (13)$$

where $\gamma_f = [(1 - r_1 r_2)/(r_1 r_2) + \alpha L]/\tau_r$, $\gamma_b = (2 - \alpha L)/\tau_r$, $A_f = \epsilon t_1/(\tau_r r_1 r_2)$, and $A_b = \epsilon t_1/(2r_1)$. The electromagnetic flux energies, I_f and I_b from the mirrors 1 and 2, respectively, are given by the squared modulus of the electric fields in the time domain. After the inverse Fourier transform, we obtain

$$\begin{aligned} I_f(\rho, t) &= I_i(\rho) |\mathcal{F}^{-1}[H_f(\omega) \tilde{g}_i(\omega + \omega_c)]|^2 = I_i(\rho) h_f(t), \\ I_b(\rho, t) &= I_i(\rho) |\mathcal{F}^{-1}[H_b(\omega) \tilde{g}_i(\omega + \omega_c)]|^2 = I_i(\rho) h_b(t), \end{aligned} \quad (14)$$

where $I_i(\rho) = 2P_i/(\pi w_0^2) e^{-2\rho^2/w_0^2}$ represents the incident intensity and P_i is the overall incident power. In summary, there are two counterpropagating optical fields that induce an absorption and consequently a local perturbation of the temperature inside the cavity, each of them depending on the incident light intensity multiplied by the transfer functions h_f and h_b . These latter can be defined as the power enhancement factors for the forward and backward fields, respectively. The absorbed power density, in the approximation of an optically thin sample, is given by [11]

$$W_{\text{abs}}(\rho, z, t) = \alpha [I_f(\rho, t)(1 - \alpha z) + I_b(\rho, t)[1 - \alpha(L - z)]]. \quad (15)$$

In CRDS experiments, the mirrors' reflectivity is quite high ($r_1, r_2 \approx 1$); this feature jointly with the optically thin sample condition leads to $H_f(\omega) \approx -H_b(\omega)$, being $\gamma_b \approx 2/\tau_r \gg |\Delta\omega|$ and $A_b \gamma_b/A_f \approx 1$. Taking into account this approximation, from Eq. (15) it emerges that W_{abs} is independent of z :

$$W_{\text{abs}}(\rho, t) \simeq \alpha I_f(\rho, t)(2 - \alpha L) \stackrel{(\alpha L \ll 1)}{\simeq} 2\alpha I_i(\rho) h_f(t). \quad (16)$$

We remind the reader that $h_f(t)$ is the squared modulus of the inverse Fourier transform of $H_f(\omega) \tilde{g}_i(\omega + \omega_c)$. The transfer function $h_f(t)$ has been calculated exactly; however, an idea of the qualitative behavior can be obtained considering that $H_f(\omega)$ is the response of the cavity to the incident field. After switching on the laser beam, the electric field E_f inside the cavity grows with an exponential law, $E_f(t) \propto e^{\gamma_f t}$ until it reaches the stationary value. Obviously, because $I_f \propto |E_f|^2$, it rises with a characteristic time $\tau_c = 1/(2\gamma_f)$. When the laser beam is switched off, the intracavity intensity decays in an exponential way with same time constant τ_c . Therefore, from Eqs. (3)–(7), (14), and (16), we obtain $\delta T_{\text{av}}(t)$ as a series of time functions, namely,

$$\delta T_{\text{av}}(t) = \frac{2}{\kappa w_0^2 L} \sum_{n=1}^{\infty} \sum_{s=0}^{\infty} A_n B_s f_{\text{ns}}(t), \quad (17)$$

$$A_n = 2\alpha \left(\int_0^L dz \phi_n(z) \right)^2, \quad (18)$$

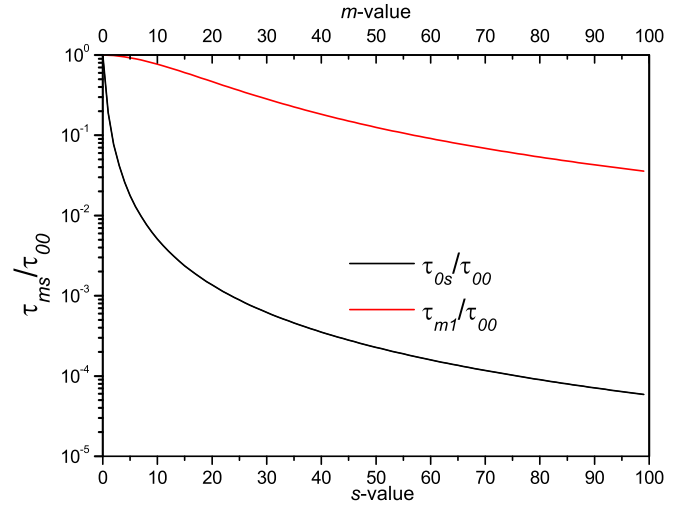


FIG. 2. Behavior of τ_{ms} as function of eigenvalue labels m and s . The values have been normalized at τ_{00} .

$$B_s = \int_0^{\rho_0} \rho' d\rho' \psi_s(\rho') \int_0^{w_0} \rho d\rho \psi_s(\rho') I_i(\rho'), \quad (19)$$

$$f_{\text{ns}}(t) = \mathcal{D} \int_{-\infty}^{\infty} dt' \theta(t - t') e^{-\mathcal{D}\beta_{\text{ns}}(t-t')} h_f(t'), \quad (20)$$

where A_n and B_s represent the overlapping coefficients between the eigenmodes of the heat equation, ψ_s and ϕ_n , with the spatial distribution of the heat source W_{abs} ; on the other hand, $f_{\text{ns}}(t)$ represents the combined effect of the temperature rise due to W_{abs} and the heat diffusion with the decay time $1/(\beta_{\text{ns}} \mathcal{D})$. After a straightforward calculation of the integrals of Eqs. (18) and (19), considering that A_n is equal to zero for even values of n and that B_s cannot be calculated analytically, we obtain

$$\delta T_{\text{av}}(t) = \frac{128\alpha P_i}{\kappa w_0^3 \rho_0 \pi^3} \sum_{m=0}^{\infty} \sum_{s=0}^{\infty} C_{ms} \hat{f}_{ms}(t), \quad (21)$$

where

$$C_{ms} = \frac{g_s J_1\left(\frac{l_s w_0}{\rho_0}\right)}{l_s J_1(l_s)^2 (2m+1)^2}, \quad (22)$$

$$g_s = \int_0^{\rho_0} \rho' d\rho' e^{-2\rho'/w_0^2} J_0\left(\frac{l_s \rho'}{\rho_0}\right), \quad (23)$$

$$\hat{f}_{ms}(t) = f_{2m+1s}(t). \quad (24)$$

In order to determine the number of eigenmodes that are needed to have a good approximation of δT_{av} , namely, $N_s \times N_m$, we calculate $\tau_{ms} = 1/(\beta_{2m+1s} \mathcal{D})$, which determines the weight of each eigenmode in the sum in Eq. (21) as a function of m and s . To this purpose, we consider the experimental configuration of Ref. [7]: $L = 50$ cm, $\rho_0 = 1$ cm, and $w_0 = 0.3$ mm. Figure 2 shows the diffusion time τ_{ms} for a variety of eigenmodes normalized to the value of τ_{00} . It is clear that τ_{00} is the bottleneck for the heat diffusion process since it gives the dominant characteristic time limiting fast heat dissipation. The value of τ_{ms} for $s \geq 20$ is about 2×10^{-3} times smaller

TABLE I. Summary of the experimental conditions of Ref. [7] used for the aims of the theoretical calculations.

Operation conditions	
Laser power, P_i	10 mW
Intracavity beam waist, w_0	0.3 mm
Mode matching parameter, ϵ^2	2.5×10^{-3}
Empty cavity finesse	$\approx 60\,000$
Mirror's radius, ρ_0	1 cm
Cavity length, L	50 cm
Gaseous medium	C_2H_2
Absorption coefficient, α (@50 Pa)	$4.22 \times 10^{-6} \text{ cm}^{-1}$

than its value at $s = 0$. In terms of m , the truncation value, N_m , has been chosen equal to 50, for which τ_{ms}/τ_{00} is about 0.1. In summary, the time evolution of $\delta T_{av}(t)$ is strictly related to three characteristic times involved in the process: Δ , τ_{00} and τ_c , which obviously depend on the experimental conditions.

III. RESULTS AND DISCUSSION

As already stated above, our model is applied to the CRDS experiment of Ref. [7], in order to quantify the possible systematic deviation arising by the local heating produced by the laser beam. Therefore, we assumed $r_1 = r_2 = 0.999975$. The sample gas is acetylene at room temperature, $T = 300$ K, with a pressure between 1 and 100 Pa. The incident wavelength is 787 nm, while the absorption coefficient per unit pressure is $\alpha_0 = 8.45 \times 10^{-8} \text{ cm}^{-1} \text{ Pa}^{-1}$. The thermal properties of acetylene adopted in our calculation are [12] $\kappa = 19.2975 \text{ mW}/(\text{m K})$, heat capacity at constant pressure $c_p = 1580 \text{ mJ}/(\text{g K})$, and thermal diffusivity given by $\mathcal{D} = \kappa/(c_p d)$, with being d the gas density. A summary of the experimental parameters values adopted in the calculation are reported in Table I. We are now ready to calculate the three characteristic times. Since $\rho_0^2 \ll L^2$ and the thermal diffusivity is inversely proportional to the gas pressures, τ_{00} can be easily found by doing the following approximation $\tau_{00} = 1/(\beta_{10}\mathcal{D}) \approx \rho_0^2 p/(l_0^2 \mathcal{D}^0)$, where p is the pressure expressed in Pa and \mathcal{D}^0 is the thermal diffusivity at the pressure of 1 Pa. If τ_{00} increases with the pressure, the cavity decay time, τ_c , has an opposite behavior with the pressure, as shown in Fig. 3. In fact, it can be easily demonstrated that the following equation holds: $\tau_c = \tau_r r_1 r_2 / [2(1 - r_1 r_2 + \alpha_0 p r_1 r_2 L)]$. It must be noted that the heat diffusion time is significantly larger than the cavity decay time, for almost the entire pressure range under investigation. Because of the strong difference between τ_c and τ_{00} , it is possible to distinguish among three different dynamical heating regimes depending on the magnitude of Δ . In order to describe the heating effect in the various regimes, we set the gas pressure at 50 Pa, thus obtaining $\tau_c = 1914 \tau_r \approx 6.4 \mu\text{s}$ and $\tau_{00} = 206786 \tau_r \approx 0.69 \text{ ms}$. Then, we calculate the behavior of $\delta T_{av}(t)$ as a function of Δ .

A. Case 1: $\Delta \ll \tau_c \ll \tau_{00}$

Equation (14) allows one to calculate analytically the function $h_f(t)$ that determines the time evolution of the in-

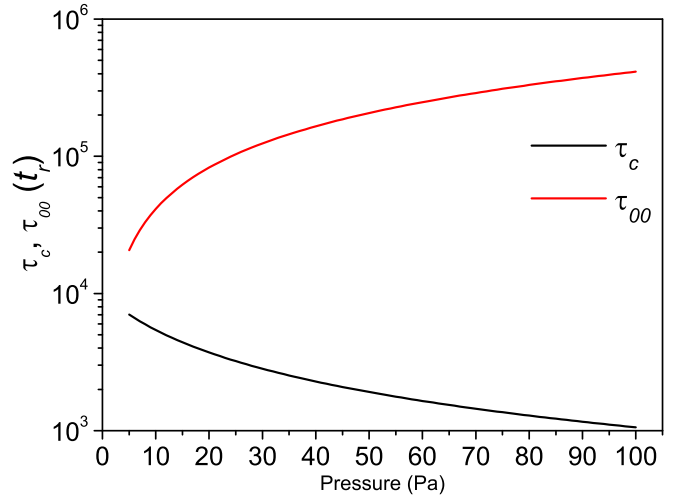


FIG. 3. Behavior of cavity time constant, τ_c , and heat diffusion time, τ_{00} , as function of gas pressure in the cavity.

tracavity heating power. For small values of t , a quadratic approximation holds for $h_f(t)$, as shown graphically in the inset of Fig. 4. This figure plots $\delta T_{av}(t)$ and $h_f(t)$ in units of Δ , assuming $\Delta = 4 \times 10^2 \tau_r$ (namely, about $1.33 \mu\text{s}$). For $t = \Delta$, $h_f(t)$ reaches its maximum value, that is, $h_f(\Delta) \approx |A_f \Delta|^2$. This value is significantly lower than we should expect when a standing wave condition is established in the cavity. As a consequence of the small intracavity power, the temperature variation, δT_{av} , does not exceed $0.57 \mu\text{K}$. Since the effective temperature variation is the mean value of $\delta T_{av}(t)$ over the time span of a few τ_c , the net effect of local heating is absolutely negligible. This is true even though the recovery time, calculated as the time to fall from 90% to 10% of the peak value of δT_{av} maximum of signal (that is, $t_{0.9} - t_{0.1}$) is relatively large, being about $60 \mu\text{s}$, and the repetition rate of the ring-down events is set at the maximum value of the order of $1/\tau_c$.

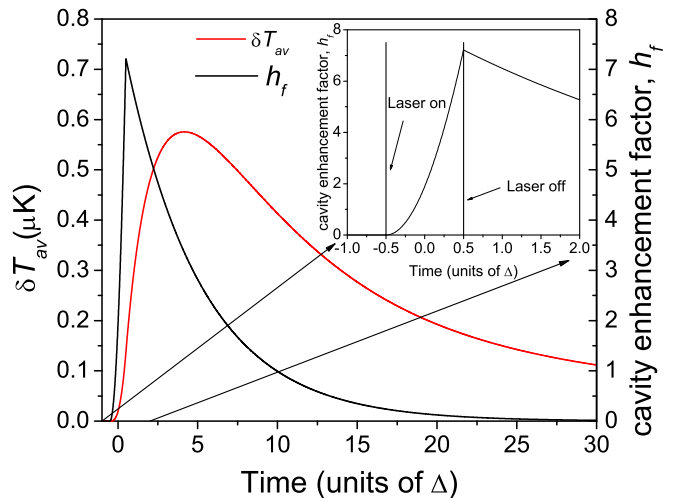


FIG. 4. Temporal dynamics of $\delta T_{av}(t)$ and $h_f(t)$ in the case of $\Delta = 4 \times 10^2 \tau_r$. The inset shows the quadratic behavior of $h_f(t)$ during the time in which the laser is on. The recovery time is about of $60 \mu\text{s}$.

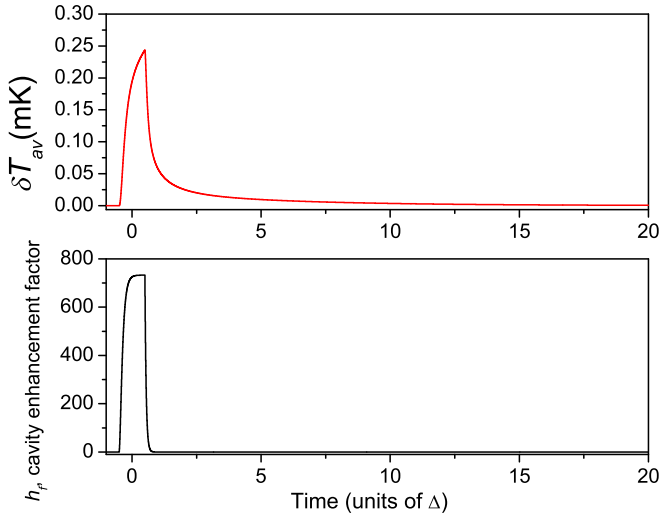


FIG. 5. Temporal dynamics of $\delta T_{av}(t)$ and $h_f(t)$ in the case of $\Delta = 4 \times 10^4 \tau_r$. The cavity enhancement factor reaches its maximum value ($|A_f/\gamma_f|^2$) that is about 730. The recovery time of $\delta T_{av}(t)$ is about 0.21 ms.

B. Case 2: $\tau_c \ll \Delta \ll \tau_{00}$

Setting $\Delta = 4 \times 10^4 \tau_r$ ($\approx 133 \mu\text{s}$), a standing wave is established inside the cavity before the laser light is switched off and the cavity enhancement factor reaches its stationary value, $h_{f\text{max}} = |A_f/\gamma_f|^2$. Heat dissipation occurs with a characteristic time much larger than Δ ; therefore $\delta T_{av}(t)$ increases up to the value of 0.24 mK, as shown in Fig. 5. The effective temperature variation is of the same order of magnitude since the mean value is calculated over a time interval during which $\delta T_{av}(t)$ exhibits a small variation.

C. Case 3: $\tau_c \ll \tau_{00} \ll \Delta$

This case is described in Fig. 6. We set $\Delta = 4 \times 10^6 \tau_r$ corresponding to about 13 ms. In this experimental condition, light absorption takes place for a long time, during which the power builds up into the cavity and the produced heat propagates throughout the medium. Therefore, δT_{av} reaches the value of 0.4 mK, thus leading to a perturbation in the gas temperature of about 1.3 ppm.

IV. CONCLUSIONS

An optical and thermal model to quantify the local heating in DBT experiments, based on the CRDS technique, has been

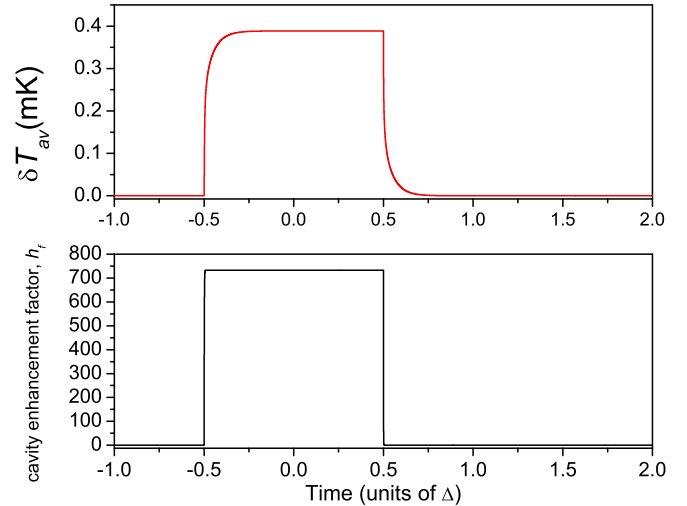


FIG. 6. Temporal dynamics of $\delta T_{av}(t)$ and $h_f(t)$ in the case of $\Delta = 4 \times 10^6 \tau_r$. The maximum deviation of temperature is 0.4 mK. The recovery time is 0.85 ms.

presented. This effect is caused by light absorption from the intracavity gaseous medium. The temperature maps have been calculated by using the Green's functions method for heat diffusion. The temperature perturbation depends on several parameters, such as the size of the optical cavity, the reflectivity of the mirrors and the thermal and optical characteristics of the probed gas. It turns out that three dynamical regimes can be identified. The worst case in terms of temperature perturbation occurs when the incident laser is switched on for a time interval that is larger than the heat diffusion time and the cavity decay time. In this condition, which is quite common in CRDS experiments, the perturbation at room temperature amounts to about 1 ppm. In each regime, the temperature perturbation increases linearly with the incident power and the absorption coefficient, which, in turn, is proportional to the gas pressure. Consequently, there might be experimental situations in which the local heating is far from being a negligible source of systematical uncertainty in Doppler broadening thermometry.

ACKNOWLEDGMENTS

This work has received funding from the EURAMET-EMPIR programme cofinanced by the Participating States and from the European Union's Horizon 2020 R&I programme through the InK2 project [13].

[1] J. Fischer, B. Fellmuth, C. Gaiser, T. Zandt, L. Pitre, F. Sparasci, M. D. Plimmer, M. de Podesta, R. Underwood, G. Sutton *et al.*, *Metrologia* **55**, R1 (2018).
 [2] L. Pitre, M. D. Plimmer, F. Sparasci, and M. E. Himbert, *C. R. Phys.* **20**, 129 (2019).
 [3] G. Machin, *Meas. Sci. Technol.* **29**, 022001 (2018).
 [4] M. R. Moldover, R. M. Gavioso, J. B. Mehl, L. Pitre, M. de Podesta, and J. T. Zhang, *Metrologia* **51**, R1 (2014).

[5] C. Gaiser, B. Fellmuth, N. Haft, A. Kuhn, B. Thiele-Krivoi, T. Zandt, J. Fischer, O. Jusko, and W. Sabuga, *Metrologia* **54**, 280 (2017).
 [6] L. Gianfrani, *Philos. Trans. R. Soc., A* **374**, 20150047 (2016).
 [7] C.-F. Cheng, J. Wang, Y. R. Sun, Y. Tan, P. Kang, and S.-M. Hu, *Metrologia* **52**, S385 (2015).
 [8] R. Gotti, L. Moretti, D. Gatti, A. Castrillo, G. Galzerano, P. Laporta, L. Gianfrani, and M. Marangoni, *Phys. Rev. A* **97**, 012512 (2018).

- [9] E. Economou, Time-independent Green's functions, *Green's Functions in Quantum Physics*, Springer Series in Solid-State Sciences (Springer, Berlin, 2006), pp. 3–19.
- [10] D. Romanini, I. Ventrillard, G. Méjean, J. Morville, and E. Kerstel, Introduction to cavity enhanced absorption spectroscopy, in *Cavity-Enhanced Spectroscopy and Sensing*, edited by G. Gagliardi and H.-P. Loock (Springer, Berlin, 2014), pp. 1–60.
- [11] B. S. Yilbas, in *Laser Heating Applications*, edited by B. S. Yilbas (Elsevier, Boston, 2012), pp. 7–51.
- [12] Gas encyclopedia air liquide, <https://encyclopedia.airliquide.com/>.
- [13] <https://www.vtt.fi/sites/InK2>.